

RESEARCH ARTICLE

Open Access



Adjacent-level biomechanics after single-level anterior cervical interbody fusion with anchored zero-profile spacer versus cage-plate construct: a finite element study

Xin-Feng Li^{1*†}, Lin-Yu Jin^{2†}, Chao-Ge Liang³, Hong-Ling Yin^{4*} and Xiao-Xing Song^{5*}

Abstract

Background: The development of adjacent segment degeneration (ASD) following ACDF is well established. There is no analytical study related to effects of plate profile on the biomechanics of the adjacent-level after ACDF. This study aimed to test the effects of plate profile on the adjacent-level biomechanics after single-level anterior cervical discectomy and fusion (ACDF).

Methods: A three-dimensional finite element model (FEM) of an intact C2–T1 segment was built and validated. From this intact model, two instrumentation models were constructed with the anchored zero-profile spacer or the standard plate-interbody spacer after a C5–C6 corpectomy and fusion. Motion patterns, the stresses in the disc, the endplate, and the facet joint at the levels cephalad and caudal to the fusion were assessed.

Results: Compared with the normal condition, the biomechanical responses in the adjacent levels were increased after fusion. Relative to the intact model, the average increase of range of motion (ROM) and stresses in the endplate, the disc, and the facet of the zero-profile spacer fusion model were slightly lower than that of the standard plate-interbody spacer fusion model. The kinematics ROM and stress variations above fusion segment were larger than that below. The biomechanical features of the adjacent segment after fusion were most affected during extension.

Conclusions: The FE analysis indicated that plate profile may have an impact on the biomechanics of the adjacent-level after a single-level ACDF. The impact may be long-term and cumulative. The current findings may help explain the decreasing incidence of ASD complications in the patients using zero-profile spacer compared with the patients using cage and plate construct.

Keywords: Cervical spine, Adjacent segment degeneration, Anterior cervical discectomy and fusion, Plate profile, Finite element analysis

* Correspondence: lxfrnji@126.com; hlyin@sjtu.edu.cn; littlestar77@126.com

[†]Xin-Feng Li and Lin-Yu Jin are Co-first author

¹Department of Orthopaedic Surgery, Baoshan Branch of Renji Hospital, School of Medicine, Shanghai Jiaotong University, No. 1058, Huan Zheng Bei Rd, Shanghai 200444, P.R. China

⁴School of Materials Science and Engineering, Shanghai Jiaotong University, No. 1954, Huashan Rd, Shanghai 20030, P.R. China

⁵Department of Anesthesiology, Ruijin Hospital, Shanghai Jiaotong University School of Medicine, 197 Ruijin Er Lu, Shanghai 200025, China

Full list of author information is available at the end of the article



© The Author(s). 2020 **Open Access** This article is licensed under a Creative Commons Attribution 4.0 International License, which permits use, sharing, adaptation, distribution and reproduction in any medium or format, as long as you give appropriate credit to the original author(s) and the source, provide a link to the Creative Commons licence, and indicate if changes were made. The images or other third party material in this article are included in the article's Creative Commons licence, unless indicated otherwise in a credit line to the material. If material is not included in the article's Creative Commons licence and your intended use is not permitted by statutory regulation or exceeds the permitted use, you will need to obtain permission directly from the copyright holder. To view a copy of this licence, visit <http://creativecommons.org/licenses/by/4.0/>. The Creative Commons Public Domain Dedication waiver (<http://creativecommons.org/publicdomain/zero/1.0/>) applies to the data made available in this article, unless otherwise stated in a credit line to the data.

Background

Anterior cervical decompression and fusion (ACDF) is a standard procedure, which can achieve good to excellent clinical results in the treatment of cervical radiculopathy and myelopathy [1–5]. Anterior stabilization techniques have been described since 1970 [6], however, the development of adjacent segment degeneration (ASD) following ACDF is well established, and ASD approximately occurs in 25% of patients within the first 10 years following fusion [7–13]

Currently, either bone or cage spacer with anterior plate and screw stabilization is the standard fusion procedure during ACDF. Although the pathogenesis of this subsequent ASD remains unknown, the development of ASD might be multifactorial. ASD changes may be related to the biomechanical effects of cervical fusion and/or the biology of cervical degeneration [11, 14–16]. After fusion, the altered biomechanics at the adjacent levels could lead to increased mobility [17–20], increased loading [21], or increased intradiscal pressure [9, 22], and, ultimately, accelerated disc degeneration [23–25].

Cage and plate construct or stand-alone cage is a popular procedure used in ACDF procedure. Recent clinical observation showed a higher incidence of ASD in ACDF with plate and cage construct (PCC) than that in stand-alone cage [26]. Clinical risk-Factor analysis of ASD following ACDF indicated that plate-to-disc distance might be an independent predisposing factor for the occurrence of ASD [27–31]. However, there is no good analytical study related to the effect of plate profile on the biomechanics of the adjacent-level after ACDF. An anchored zero-profile spacer (Zero-P) has been developed to reduce the potential risk of complications after anterior cervical fusion with plating. To clarify the effect of plate profile on the biomechanics of the adjacent-level after ACDF, the present study aimed to observe the different biomechanical features of the adjacent segment after fusion with the Zero-P and the PCC.

Methods

Study design

In this study, a computational biomechanical analysis was used to describe and predict the effect of plate profile on the mechanical behavior of the adjacent segment after ACDF.

Development of finite element model (FEM)

A 3-dimensional FEM of a normal C2-T1 segment was created in this study. A 38-year-old male patient was selected in our simulation. This study was performed in accordance with the ethical standards of the Institutional Ethics Committee of our hospital. Written informed consent was obtained from the patient. The model was developed from the computed tomographic (CT) scan of

this male subject. Model creating methods were used as we previously described [32–35]. Lordosis of C2-C7 in current model was 23.7°. The measured Cobb angle was in the reported range of the subaxial cervical spine [36]. The global xyz coordinate system was set with the positive z-axis acting along the rostral-caudal extent of the spine pointing up, the positive x-axis was perpendicular to the z-axis pointing right, and the positive y-axis was perpendicular to the x-axis and z-axis pointing backward. The model components included cortical bone, cancellous bone, bony posterior elements, annulus fibrosus (AF), nucleus pulposus (NP), posterior facets, end plates, anterior longitudinal ligament, posterior longitudinal ligament, ligamentum flavum, interspinous ligament, and capsular ligaments. The material properties were assumed to be homogeneous and isotropic according to the published literature [37–42]. The annular fibers embedded in the ground substance were assembled in a crisscross manner. The facet joint was created as a nonlinear three-dimensional contact problem using surface-to-surface contact elements. Surface to surface contact algorithm is used in defining facet joint interaction and friction coefficient was assumed to be 0.1 [43]. The initial material properties were based on previous studies as shown in Table 1.

Model validation

Range of motion (ROM) of each cervical segment was the major indicator for FEM validation. Subaxial ROM and functional spinal unit ROM were calculated. The subaxial ROM was defined as the measurement of the total motion between the C2 and C7 vertebrae. The functional spinal unit ROM, intersegmental motion, was the motion between two adjacent vertebrae. The predicted ROM (movement in sagittal plane, coronal plane and axial plane) were compared with the in vivo and in vitro data obtained from healthy normal cervical spine [44–47]. All simulations had the same boundary and loading conditions with the controlled experimental studies. Boundary conditions, defined as the inferior surface of T1 vertebra was fully constrained in all loading conditions. To simulate the upper head weight, a compressive preload of 100 N was applied to simulate physiologic compressive loads [42, 44]. The compressive preload was applied using the follower load technique [48]. After applying the preload, a 2-Nm bending moment was applied to the superior surface of C2. Simulations were conducted using Abaqus (Simulia, Providence, RI). Subaxial ROM and functional spinal unit ROM were recorded.

Fusion models simulation and biomechanical changes

Fusion models were developed from the intact cervical spine model. Discectomy and accommodate the

Table 1 Material properties of the spinal structures and instrumentations

Description	Element Type	Young's Modulus (MPa) E	Poisson Ratio μ	Cross Sectional Area (mm ²)
Cortical bone	Shell elements	12,000	0.29	–
Cancellous bone	3-D solid elements (4 node)	450	0.25	–
Facet cartilage	3-D solid elements (4 node)	10.4	0.4	–
Annulus fibers	3-D solid elements (8 node)	48	0.4	–
Nucleus pulposus	3-D solid elements (8 node)	1.0	0.49	–
Endplate	3-D solid elements	500	0.4	–
Anterior longitudinal ligament	3-D tension truss elements	30	0.3	33
Posterior longitudinal ligament	3-D tension truss elements	20	0.3	33
Interspinous ligament	3-D tension truss elements	1.5	0.39	13
Ligamentum flavum	3-D tension truss elements	5	0.3	50.1
Capsular ligaments	3-D tension truss elements	20	0.3	46.6
PEEK cage	3-D solid elements (4 node)	3600	0.3	–
Titanium plate	3-D solid elements (4 node)	110,000	0.3	–
Screw	3-D solid elements (4 node)	110,000	0.3	–

implant-bone graft assembly were simulated. To simulate single-level ACDF, the anterior longitudinal ligament, the C5-C6 intervertebral disc and cartilaginous endplate were removed, keeping posterior elements, associated ligaments and facet surfaces, and uncovertebral joints intact. Three conditions were modeled: intact model, 4-screw anchored Zero-P fusion model (ZeroP, DePuy Synthes Spine, Raynham, Massachusetts), and the standard PCC fusion model. The screw-plate and screw-bone interface were completely fixed in all directions. In the standard PCC, a rigid anterior cervical plate was used, plate (width 16 mm, thickness 2 mm) and fixed screws (diameter 4 mm, length 14 mm) were rigidly fixed in the operative segment. To maintain the sagittal alignment after surgery, the same PEEK interbody spacer (width 15 mm, length 16 mm, and height 6 mm) was used. Cervical spine alignment was assessed with the C2–7 Cobb angle. The angle was 22° for both fusion models. To simulate a standard surgical procedure, we placed the plate at least 5 mm away from the adjacent disc spaces. The above and below distance of the plate to the adjacent disc were 5.5 mm and 5 mm in PCC model, whereas, 13.5 mm and 12.5 mm in anchored Zero-P model. In the Zero-P system, fixed screws (diameter 3 mm, length 16 mm) were adopted. The titanium alloy plate and PEEK material properties were assigned to the respective implants (Table 1). Biomechanical segmental response in different model conditions was simulated. A torque of 2 Nm was applied with a 100-N axial preload. The inferior surface of T1 was fully constrained along three perpendicular planes in all loading conditions. The biomechanical responses of adjacent segments at the cephalad and caudal levels of the operation level were assessed in terms of ROM, stresses in the endplate,

disc and facet. ROM in sagittal plane, coronal plane and axial plane was measured. Stresses were calculated using the average von-Mises stresses. The facet stresses at a motion segment was defined as the average von-Mises stresses on the right and left articulating facets.

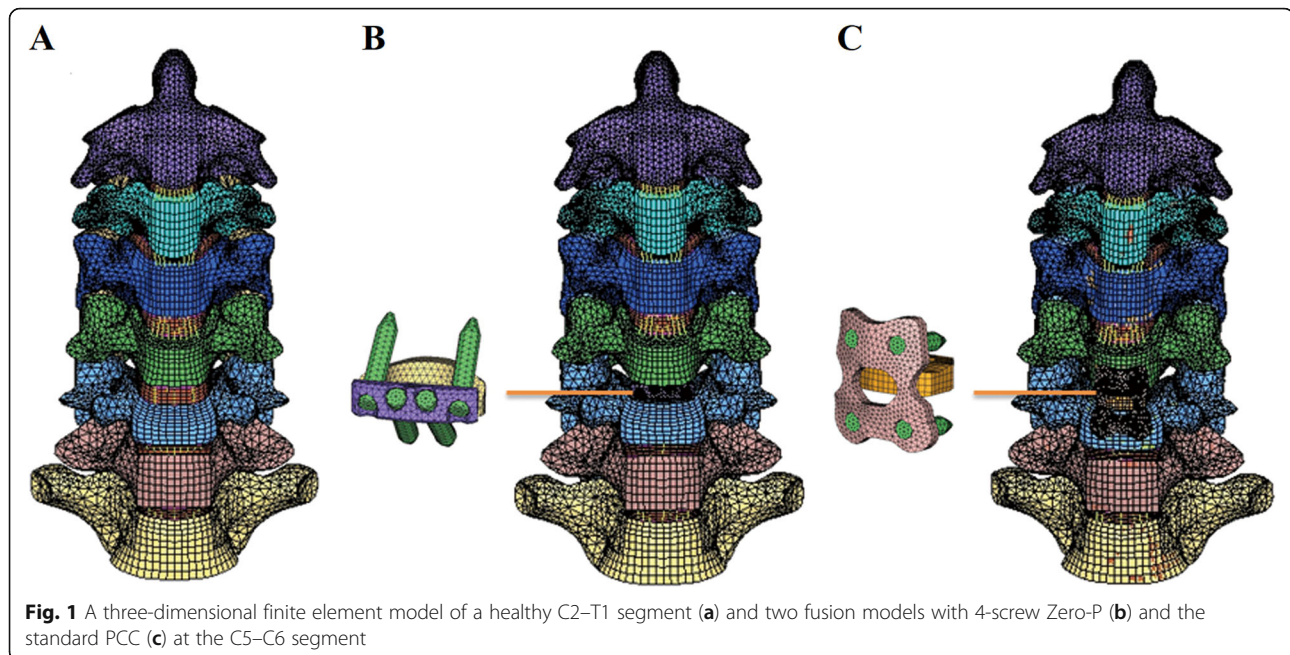
Results

Model validation

The intact cervical spine FEM consisted of 152,608 elements and 41,797 nodes (Fig. 1a). The validation studies of the current FEM were shown in Figs. 2 and 3. Comparison of the total subaxial ROM was displayed in Fig. 2. The kinematic response of each segment of the FEM was compared with the corresponding in vivo and in vitro data [44–47] (Fig. 3). The total subaxial ROM of the normal FEM in the sagittal, the transverse, and the frontal planes were 72°, 32°, and 47° respectively. The segmental motions predicted by the normal C2–T1 FEM in the sagittal plane, transverse plane, and the frontal plane respectively were as follows: C2–C3 (10.8°, 3.5°, 10.8°), C3–C4 (12.8°, 4.8°, 12.2°), C4–C5 (13.5°, 7.5°, 12.5°), C5–C6 (14.0°, 7.4°, 10.0°), C6–C7 (12.4°, 7.1°, 4.1°), and C7–T1 (6.5°, 5.6°, 1.3°). The motions obtained from the present FEM were within standard deviation of the in vitro or in vivo study. The differences in segmental motions between the intact FEM and in vitro or in vivo data were small. Following validation, the C2–T1 FEM was then used to understand the biomechanical effects of plate profile on the biomechanical changes in adjacent segments (Fig. 1).

Kinematics changes in the adjacent segments after fusion

Kinematics changes relative to intact condition in the adjacent segment ROM, both at the proximal (Fig. 4a)



and distal (Fig. 4b) adjacent levels were demonstrated. The ROM in both adjacent segments was greater after fusion than that in intact model. The highest increase was observed in the standard PCC fusion model, followed by the Zero-P fusion model. Compared with the intact model, the motions in the instrumentation models increased at segments adjacent to the fusion construct (C4–C5, C6–C7): the Zero-P fusion model (flexion-extension [29, 17%], axial rotation [8, 6%] and lateral bending [26, 10%]); and the PCC fusion model (flexion-extension [37, 22%], axial rotation [13, 9%] and lateral bending [35, 16%]). Motion changes were higher at the proximal adjacent levels than at the distal adjacent levels in the sagittal plane, the axial plane and the frontal plane. Both in the Zero-P fusion model and in the PCC fusion model, the motion of superior and inferior adjacent levels was most affected during movement in the sagittal plane.

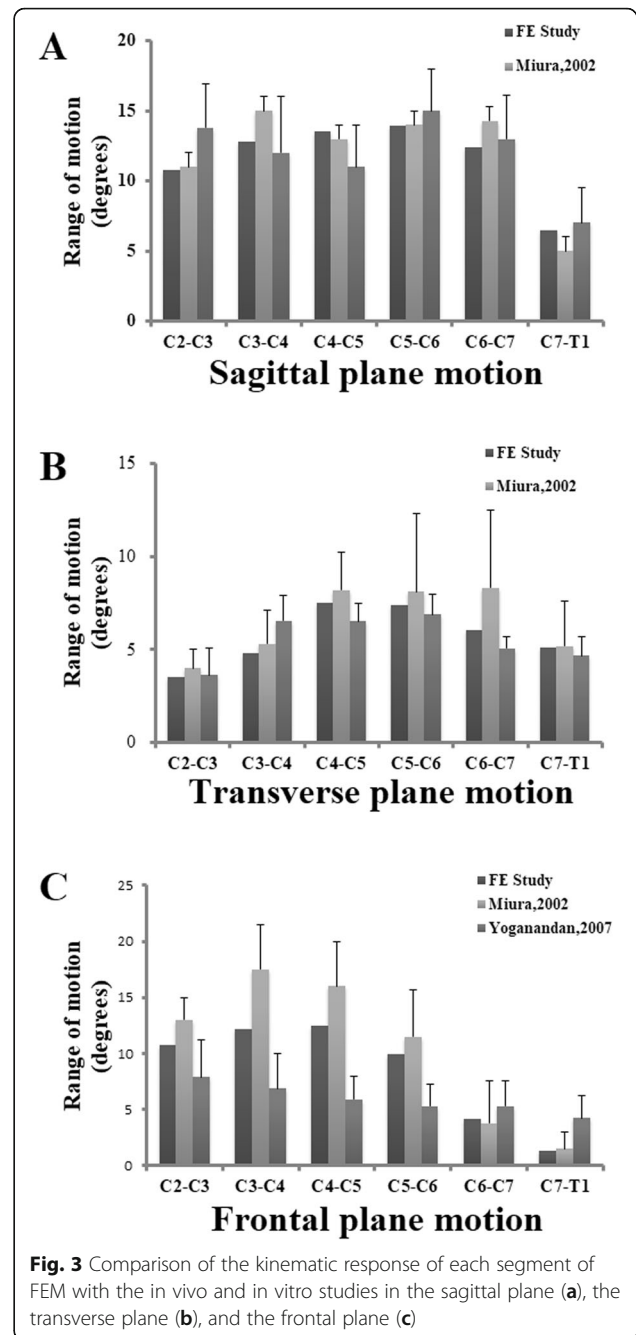
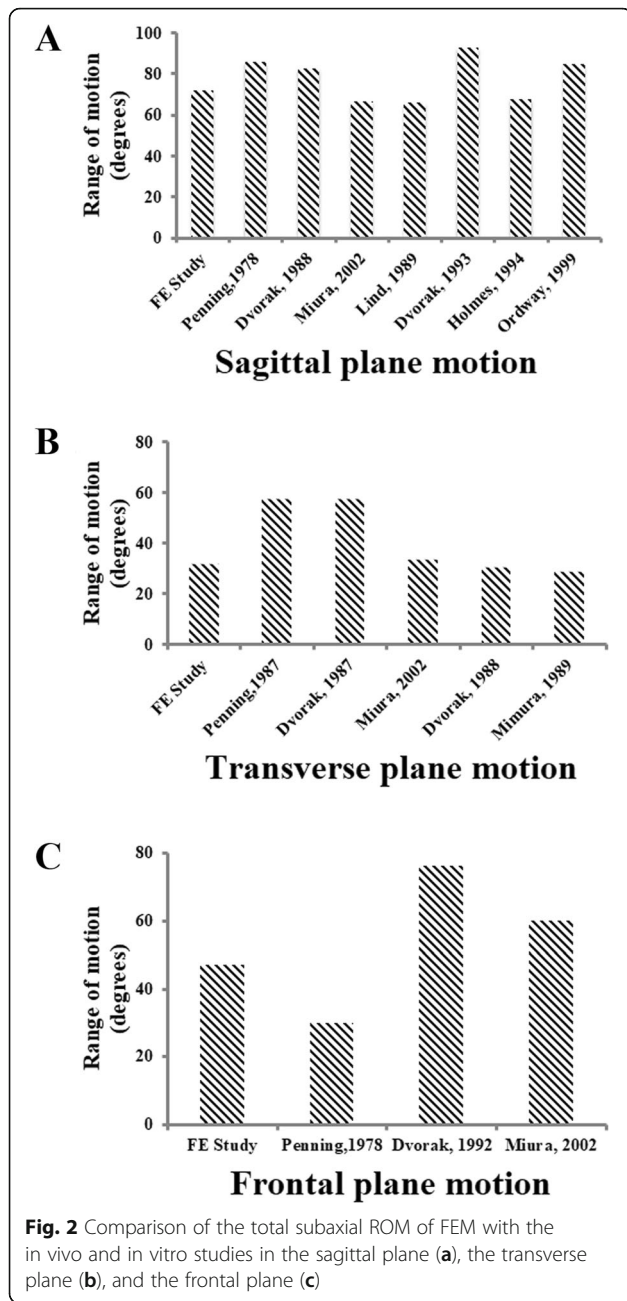
Intradiscal stress changes in the adjacent level

As shown in Fig. 5, compared with the intact model, the average disc stresses at the segments adjacent to the fusion construct (C4–C5, C6–C7) increased both in two instrumentation models. The disc stress increase in the fusion models was generally greater in the superior C4–C5 disc than that in the inferior C6–C7 disc during extension, axial rotation and lateral bending movement. In the C4–C5 disc, relative to the intact model, the average disc stress in the Zero-P and the PCC fusion model, increased by 21 and 24% during flexion; 64 and 66% during extension; 1 and 3% during axial rotation; and 5 and

6% during lateral bending. In the C6–C7 disc, when compared with the intact model, the average disc stress for Zero-P and PCC fusion model was 37 and 39% larger in flexion; 59 and 63% larger in extension; 2 and 2% larger in axial rotation; and 2 and 4% larger in lateral bending (Fig. 5b). Stresses of the superior C4–C5 and inferior C6–C7 discs were most affected in extension (Fig. 5). Intradiscal stress distribution features of C4–C5 and C6–C7 segments in the intact model, Zero-P model and PCC model under flexion, extension, axial rotation and lateral bending conditions were presented in Fig. 6. The maximum von Mises stress occurred at the anterior part of AF in flexion, at the posterolateral part in extension and at the lateral part in axial rotation and lateral bending movement.

End-plate stress changes in the adjacent segments

The C5 superior and C6 inferior end-plate stresses of two fusion models were higher than those of the intact model as shown in Fig. 7. In the fusion models, the end-plate stresses were highest during extension. The differences of the end-plate stresses between two fusion models were lowest during rotation. The increased stress values of C5 inferior end-plate relative to the intact model in the Zero-P fusion model were lower than that in the PCC fusion model in flexion (28, 33%), extension (113, 119%), and lateral bending (13, 30%). The increased stress values of C6 inferior endplate relative to the intact model in the Zero-P fusion model were also lower than that in the PCC fusion model in flexion (27, 32%), extension (90, 98%), and lateral bending (7, 28%).



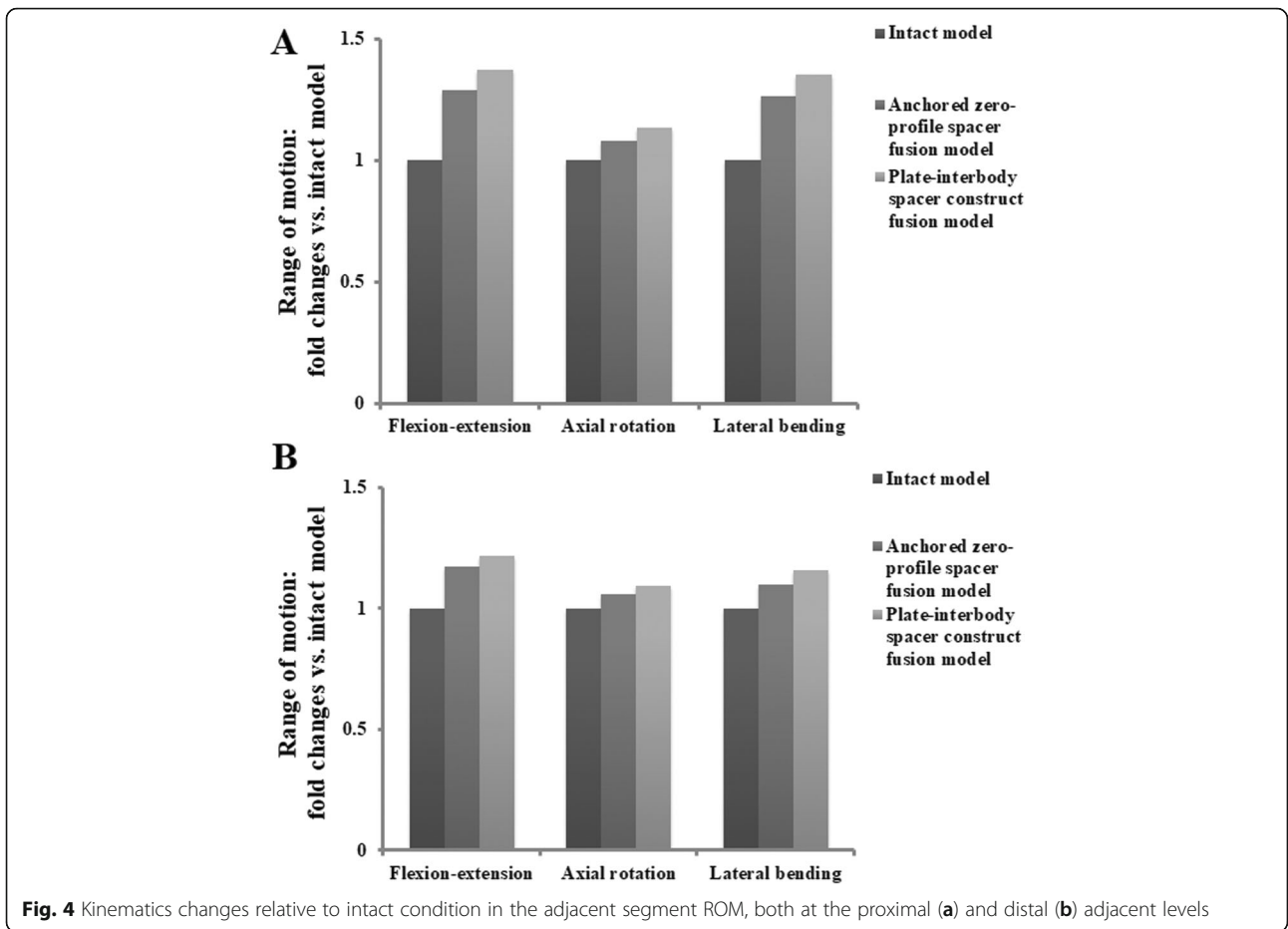
Facet load changes in the adjacent level

The stress in the facet was found to be the greatest in two fusion models (Fig. 8). Compared with the intact model, the facet stress in the instrumentation models increased at the segments adjacent to the fusion construct (C4–C5, C6–C7): the zero-profile spacer fusion model (flexion [49, 40%], extension [102, 97%], axial rotation [48, 38%], and lateral bending [57, 26%]); the PCC fusion model (flexion [71, 52%], extension [117, 111%], axial rotation [48, 36%], and lateral bending [77, 39%]). The increased stress in the facet relative to the intact model was higher in the superior C4–C5 segment than in the

inferior C6–C7 segment during flexion, extension, and lateral bending. The stresses were largest during extension.

Discussion

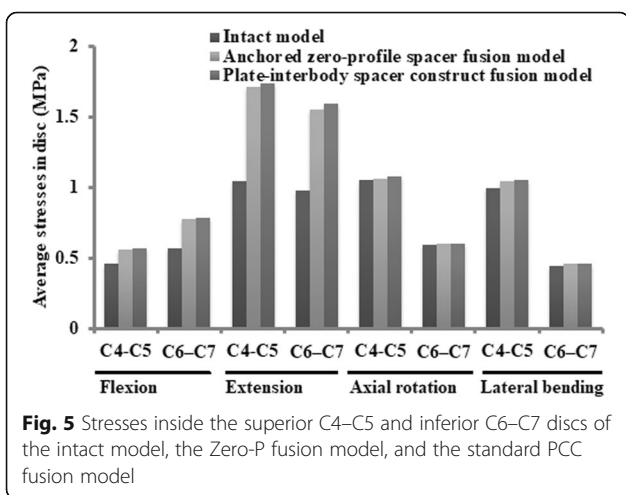
Spinal arthrodesis biomechanically transfers additional stress to the adjacent segments, which may play a role in the development of ASD. The results obtained in the current computational investigation indicated that plate profile has an impact on the biomechanics of the adjacent-level after a single-level ACDF. The

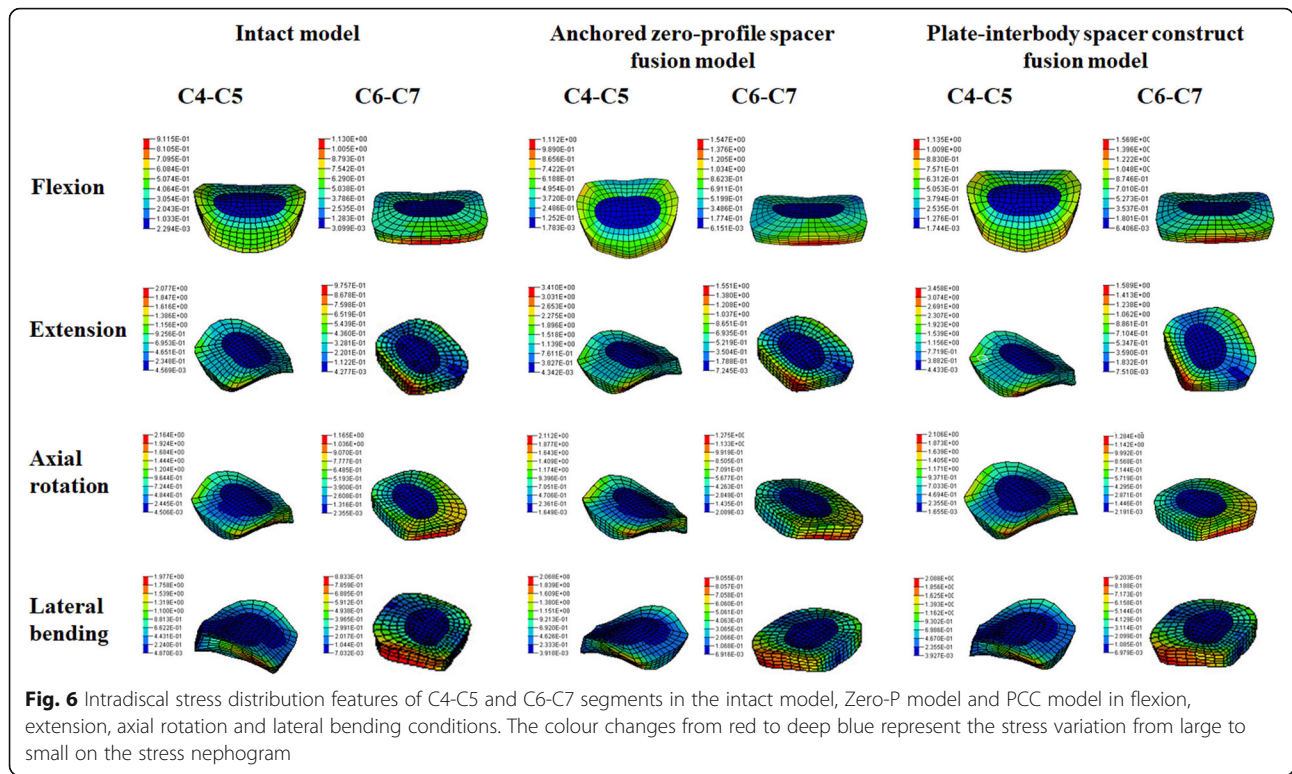


biomechanical responses in the endplate, the disc, and the facets in the adjacent levels were increased after fusion, compared with that in the intact model. Relative to the intact model, the average increase of ROM and stresses in the Zero-P fusion model were slightly lower

than that in the standard PCC fusion model during flexion, extension, and lateral bending. The kinematics ROM and stress variations above fusion segment were larger than that below. The biomechanical features of the adjacent segment after fusion were most affected during extension.

Patients with spinal fusion are at greater risk for ASD and some of them are require additional surgery. ACDF with plating has become the most popular surgical approach for treatment of cervical spine disorders because anterior plates provide many advantages than without plating. As indicated in the present finite element study, ACDF impairs normal cervical biomechanics, alters mechanics at adjacent segments, resulting in higher stress and hypermobility in adjacent segments. Our results are in line with the reported data of the biomechanical studies on the behavior of the adjacent segments in the setting of different operation procedures [49–53]. Both the present and all of the reported results suggested that ASD might be related to iatrogenic biomechanics. Although the pathophysiology of ASD remains controversial, ASD is likely a multifactorial process that is not only driven by natural history, but also affected by the

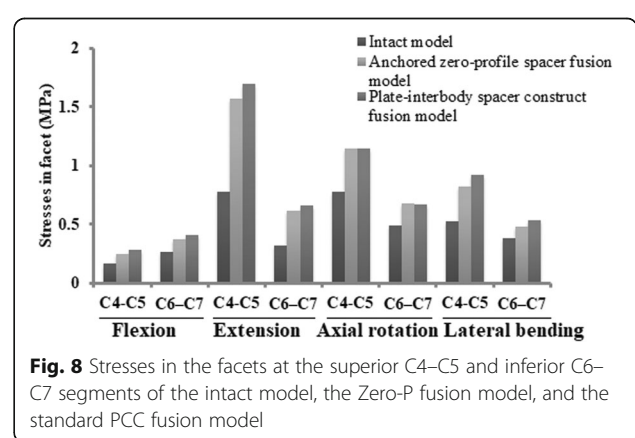
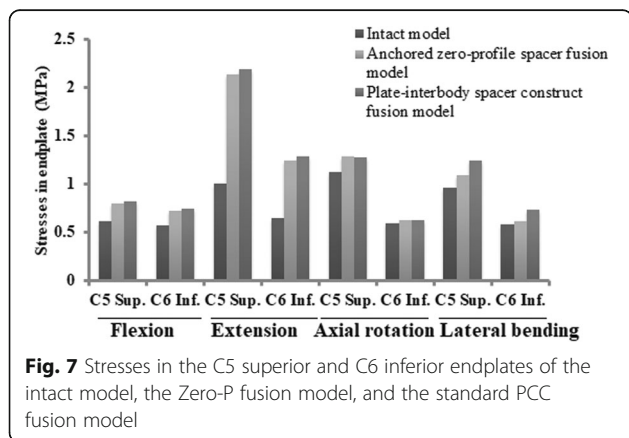




increased adjacent segment mobility and by the changes of mechanical environment [54–56]. It is well known that mechanical loads could induce intervertebral disc degeneration by initiating degeneration or by regulating cell-mediated remodeling events that occur in response to the mechanical stimuli [57]. Mechanical stimuli have an impact upon the cellular response to loading and upon changes that occur with aging and degeneration of the intervertebral disc [58, 59].

Low profile, integrated interbody cages design anchors to the vertebral bodies from within the disc space. In vitro biomechanical study showed that the anchored

cage afforded biomechanical stability comparable to that of the standard plate-interbody cage [60, 61]. This design has greater advantages in decreasing incidence of post-operative dysphagia and ASD complications. As demonstrated in several clinical studies, the Zero-P group had a significantly reduced incidence of ASD compared with the PCC group [61–67]. Our kinematics simulation study showed a lower hypermobility in adjacent segments in the Zero-P fusion model than that in the standard PCC fusion model (Fig. 4). Excessive motion of a given motion segment unit has been postulated to lead to an increased risk of disc degeneration, due to



mechanical forces exerted on adjacent segments from the longer lever arm of the fused segments might accelerate degeneration [29, 61].

ASD is defined as radiographical changes at levels adjacent to a previous spinal fusion. ASD may manifest as cervical segment degeneration, such as disc degeneration, facet hypertrophy, segmental instability, et al.. In our simulation study, the average increase in stress values in the facet joint, the disc and the endplate of the Zero-P fusion model relative to the intact model were slightly lower than that of the standard PCC fusion model during flexion, extension, and lateral bending movement (Figs. 5, 6, 7 and 8). Increased stress might induce and aggravate degeneration of cervical facet joints and disc. The endplate also plays a key role in the development of disc degeneration, because most small molecule nutrient transport occurs via the endplate [68]. Load could regulate nutrient supply via the endplate. Dysfunction of nutrition channel on cartilage endplate caused by abnormal stress intervention may be a contributory factor of cervical disc degeneration [69]. Therefore, larger stress in adjacent segments of the PCC model might lead to a higher incidence of ASD than in the Zero-P model.

Investigators have studied the risk factors for adjacent segment disease in spinal fusion. There are still disputes about the influence of plate-to-disc distance on ASD. Several clinical studies could not draw the conclusion that plate-to-disc distance affects the development of ASD [70], however, more and more studies have reported that plate-to-disc distance was independently associated with ASD, and the shortest plate is recommended to use to avoid intrusion of the plate close to the adjacent segments [27, 28, 71–73]. The Zero-P implant consists of a cage and an internal implant with a pair of locking screws. The greatest difference between the Zero-P and traditional PCC structures is that whether additional titanium alloys plate is attached to the anterior surface of the vertebral body. In the current computational simulation, at least 5 mm of plate-to-disc distance was adopted to simulate a standard ACDF surgical procedure. Our finite element study indicated that the standard PCC fusion model has a slightly larger stress transmitted to the adjacent segment than the Zero-P model. Compared to the traditional PCC model, the plate-to-disc distance in the Zero-P is longest. Therefore, the process of ASD might be influenced by the plate-to-disc distance. The biomechanical differences between the two models were small in the present study. This might be due to a single level fusion model was used in our study. The differences might be large in two or three level fusion situations.

Limitations

There are some limitations in the present study. Although extra care was taken during model development

and analysis, the finite element analysis has limitations, just like the cadaver studies and other published finite element studies. Caution should be taken when interpreting the results of the present study, because the intact FEM is based on a single scan of a normal man. The computational simulation aimed to provide the trend rather than the actual data. The comparison in the finite element analysis is not a statistical comparison. It is only a biomechanical trend analysis and comparison, similar to many finite element analysis researches. In our FEM, neck muscles were absence. The muscles mainly control the cervical range of motion. The absence of neck muscles may have some effect on the finite element biomechanical values, such as motion and stress. The fusion models were created and modified based on the healthy FEM. The cervical spine structures not to undergo surgery might be of different degenerative degree. Therefore, the conclusions of the present study should not be extrapolated to different genders or ages with varying degrees of degeneration. To improve the model and to study the effects of pre-exist degenerative changes in adjacent levels on the adjacent segment biomechanics after ACDF, mild, moderate and severe degeneration conditions should be simulated. Both the geometry and material properties should be changed. Height reduction, anterior osteophytes and endplate sclerosis should be incorporated into the geometry changes of different degeneration as the clinical basis. In addition to changing the geometry of the disc and the nucleus with altered mechanical properties, the FEM also includes changes in the permeability and porosity of various disc components and the reduction in nucleus water content. The effects of degenerative changes in adjacent levels on the biomechanical response of adjacent segment after ACDF should be studied further.

Conclusion

In summary, this study showed that the ACDF, either with the Zero-P or with the standard PCC, could induce higher changes in the adjacent segment flexibility and in the disc, the endplate, and the facet stresses compared with the normal condition. Biomechanical factors related to the development of ASD progression are highest in the segment immediately above the fusion. The biomechanical features of the adjacent segment after fusion were most affected during extension. The finite element analysis indicated that the plate profile might affect the biomechanics of the adjacent-level after a single-level ACDF. The average increase of ROM and stress in the PCC model were slightly larger than that in the Zero-P model. The current findings may help explain the decreasing incidence of ASD complications in the patients using Zero-P compared with the patients using PCC.

Abbreviations

ASD: Adjacent segment degeneration; ACDF: Anterior cervical decompression and fusion; FEM: Finite element model; ROM: Range of motion; Zero-P: Zero-profile spacer; PCC: Plate and cage construct; AF: Annulus fibrosus; NP: Nucleus pulposus

Acknowledgements

We are grateful to all study participants for their participation in the study.

Authors' contributions

Conceived and designed the experiments: XFL, LYJ, XXS. Performed the experiments: XFL, LYJ, HLY. Analyzed the data: XFL, LYJ, CGL, HLY. Wrote the paper: XFL, LYJ, HLY, XXS. All authors read and approved the final manuscript.

Funding

This study was supported by the National Natural Science Foundation of China (81772292, 81270027) and by Medico-Engineering cooperation Fund of Shanghai Jiao Tong University (No. YG2012MS25, No. YG2016MS54). The funding bodies did not have any role in the study design, the data collection, the analyses, the interpretation of data or the writing of the manuscript.

Availability of data and materials

The datasets used and/or analyzed during the current study are available from the corresponding author on reasonable request.

Ethics approval and consent to participate

This study was performed in accordance with the ethical standards of the Institutional Ethics Committee of Baoshan branch of Renji hospital and in accordance with the 1964 Declaration of Helsinki and its later amendments or comparable ethical standards. The participant provided written consent to participate in our study.

Consent for publication

Written consent for publication was obtained from the participant described in this article.

Competing interests

The authors declare that they have no competing interests.

Author details

¹Department of Orthopaedic Surgery, Baoshan Branch of Renji Hospital, School of Medicine, Shanghai Jiaotong University, No. 1058, Huan Zheng Bei Rd, Shanghai 200444, P.R. China. ²Department of Spinal Surgery, Peking University People's Hospital, Peking University, Beijing 100044, China. ³Department of Orthopaedic Surgery, Shanghai Xijiao Orthopaedic Hospital, Shanghai 200336, China. ⁴School of Materials Science and Engineering, Shanghai Jiaotong University, No. 1954, Huashan Rd, Shanghai 20030, P.R. China. ⁵Department of Anesthesiology, Ruijin Hospital, Shanghai Jiaotong University School of Medicine, 197 Ruijin Er Lu, Shanghai 200025, China.

Received: 12 January 2020 Accepted: 25 March 2020

Published online: 06 April 2020

References

- Smith GW, Robinson RA. The treatment of certain cervical-spine disorders by anterior removal of the intervertebral disc and interbody fusion. *J Bone Joint Surg Am.* 1958;40-a(3):607–24.
- Cloward RB. The anterior approach for removal of ruptured cervical disks. *J Neurosurg.* 1958;15(6):602–17.
- Robinson RA. The problem of neck pain: its alleviation by anterior removal of intervertebral disc with interbody fusion in the cervical spine. *J Med Assoc State Ala.* 1963;33:1–14.
- Burkhardt BW, Brielmaier M, Schwerdtfeger K, Sharif S, Oertel JM. Smith-Robinson procedure with and without Caspar plating as a treatment for cervical spondylotic myelopathy: a 26-year follow-up of 23 patients. *Eur Spine J.* 2017;26(4):1246–53.
- Brodke DS, Zdeblick TA. Modified Smith-Robinson procedure for anterior cervical discectomy and fusion. *Spine (Phila Pa 1976).* 1992;17(10 Suppl):S427–30.
- Schürmann K, Busch G. Treatment of cervical dislocation fractures using ventral fusion. *Der Chirurg; Zeitschrift für alle Gebiete der operativen Medizen.* 1970;41(5):225–8.
- Carrier CS, Bono CM, Lebl DR. Evidence-based analysis of adjacent segment degeneration and disease after ACDF: a systematic review. *Spine J.* 2013; 13(10):1370–8.
- Cho SK, Riew KD. Adjacent segment disease following cervical spine surgery. *J Am Acad Orthop Surg.* 2013;21(1):3–11.
- Eck JC, Humphreys SC, Lim TH, Jeong ST, Kim JG, Hodges SD, An HS. Biomechanical study on the effect of cervical spine fusion on adjacent-level intradiscal pressure and segmental motion. *Spine (Phila Pa 1976).* 2002; 27(22):2431–4.
- Hilibrand AS, Robbins M. Adjacent segment degeneration and adjacent segment disease: the consequences of spinal fusion? *Spine J.* 2004;4(6 Suppl):190s–4s.
- Lawrence BD, Hilibrand AS, Brodt ED, Dettori JR, Brodke DS. Predicting the risk of adjacent segment pathology in the cervical spine: a systematic review. *Spine (Phila Pa 1976).* 2012;37(22 Suppl):S52–64.
- Matsumoto M, Okada E, Ichihara D, Watanabe K, Chiba K, Toyama Y, Fujiwara H, Momoshima S, Nishiwaki Y, Iwanami A, et al. Anterior cervical decompression and fusion accelerates adjacent segment degeneration: comparison with asymptomatic volunteers in a ten-year magnetic resonance imaging follow-up study. *Spine (Phila Pa 1976).* 2010;35(1):36–43.
- Song JS, Choi BW, Song KJ. Risk factors for the development of adjacent segment disease following anterior cervical arthrodesis for degenerative cervical disease: comparison between fusion methods. *J Clin Neurosci.* 2014; 21(5):794–8.
- Asghar FA. Radiographic Changes in the Cervical Spine Following Arthrodesis: Causation or Correlation? Commentary on an article by Raj D. Rao, MD, et al: "Radiographic Changes in the Cervical Spine Following Anterior Arthrodesis: A Long-Term Analysis of 166 Patients". *J Bone Joint Surg Am.* 2016;98(19):e85.
- Lee MJ, Dettori JR, Standaert CJ, Ely CG, Chapman JR. Indication for spinal fusion and the risk of adjacent segment pathology: does reason for fusion affect risk? A systematic review. *Spine (Phila Pa 1976).* 2012;37(22 Suppl):S40–51.
- van Eck CF, Regan C, Donaldson WF, Kang JD, Lee JY. The revision rate and occurrence of adjacent segment disease after anterior cervical discectomy and fusion: a study of 672 consecutive patients. *Spine (Phila Pa 1976).* 2014; 39(26):2143–7.
- Clements DH, O'Leary PF. Anterior cervical discectomy and fusion. *Spine (Phila Pa 1976).* 1990;15(10):1023–5.
- Baba H, Furusawa N, Imura S, Kawahara N, Tsuchiya H, Tomita K. Late radiographic findings after anterior cervical fusion for spondylotic myeloradiculopathy. *Spine (Phila Pa 1976).* 1993;18(15):2167–73.
- Anderson PA, Sasso RC, Hipp J, Norvell DC, Raich A, Hashimoto R. Kinematics of the cervical adjacent segments after disc arthroplasty compared with anterior discectomy and fusion: a systematic review and meta-analysis. *Spine (Phila Pa 1976).* 2012;37(22 Suppl):S85–95.
- Dong L, Xu Z, Chen X, Wang D, Li D, Liu T, Hao D. The change of adjacent segment after cervical disc arthroplasty compared with anterior cervical discectomy and fusion: a meta-analysis of randomized controlled trials. *Spine J.* 2017;17(10):1549–58.
- Matsunaga S, Kabayama S, Yamamoto T, Yone K, Sakou T, Nakanishi K. Strain on intervertebral discs after anterior cervical decompression and fusion. *Spine (Phila Pa 1976).* 1999;24(7):670–5.
- Pospiech J, Stolke D, Wilke HJ, Claes LE. Intradiscal pressure recordings in the cervical spine. *Neurosurgery.* 1999;44(2):379–84 discussion 384–375.
- Maiman DJ, Kumaresan S, Yoganandan N, Pintar FA. Biomechanical effect of anterior cervical spine fusion on adjacent segments. *Biomed Mater Eng.* 1999;9(1):27–38.
- Schwab JS, Diangelo DJ, Foley KT. Motion compensation associated with single-level cervical fusion: where does the lost motion go? *Spine (Phila Pa 1976).* 2006;31(21):2439–48.
- Ragab AA, Escarcega AJ, Zdeblick TA. A quantitative analysis of strain at adjacent segments after segmental immobilization of the cervical spine. *J Spinal Disord Tech.* 2006;19(6):407–10.
- Ji GY, Oh CH, Shin DA, Ha Y, Kim KN, Yoon DH, Yudoyono F. Stand-alone cervical cages versus anterior cervical plates in 2-level cervical anterior interbody fusion patients: analysis of adjacent segment degeneration. *J Spinal Disord Tech.* 2015;28(7):E433–8.

27. Park JB, Cho YS, Riew KD. Development of adjacent-level ossification in patients with an anterior cervical plate. *J Bone Joint Surg Am.* 2005;87(3):558–63.
28. Chung JY, Kim SK, Jung ST, Lee KB. Clinical adjacent-segment pathology after anterior cervical discectomy and fusion: results after a minimum of 10-year follow-up. *Spine J.* 2014;14(10):2290–8.
29. Yang H, Lu X, He H, Yuan W, Wang X, Liao X, Chen D. Longer plate-to-disc distance prevents adjacent-level ossification development but does not influence adjacent-segment degeneration. *Spine (Phila Pa 1976).* 2015;40(7):E388–93.
30. Lee DH, Lee JS, Yi JS, Cho W, Zebala LP, Riew KD. Anterior cervical plating technique to prevent adjacent-level ossification development. *Spine J.* 2013;13(7):823–9.
31. Chung JY, Park JB, Seo HY, Kim SK. Adjacent segment pathology after anterior cervical fusion. *Asian Spine J.* 2016;10(3):582–92.
32. Li XF, Dai LY. Acute central cord syndrome: injury mechanisms and stress features. *Spine (Phila Pa 1976).* 2010;35(19):E955–64.
33. Li XF, Dai LY. Three-dimensional finite element model of the cervical spinal cord: preliminary results of injury mechanism analysis. *Spine (Phila Pa 1976).* 2009;34(11):1140–7.
34. Li XF, Liu ZD, Dai LY, Zhong GB, Zang WP. Dynamic response of the idiopathic scoliotic spine to axial cyclic loads. *Spine (Phila Pa 1976).* 2011;36(7):521–8.
35. Song XX, Jin LY, Li XF, Qian L, Shen HX, Liu ZD, Yu BW. Effects of low bone mineral status on biomechanical characteristics in idiopathic scoliotic spinal deformity. *World Neurosurg.* 2018;110:e321–9.
36. Linder A. A new mathematical neck model for a low-velocity rear-end impact dummy: evaluation of components influencing head kinematics. *Accid Anal Prev.* 2000;32(2):261–9.
37. Yoganandan N, Kumaresan S, Pintar FA. Geometric and mechanical properties of human cervical spine ligaments. *J Biomech Eng.* 2000;122(6):623–9.
38. Yoganandan N, Kumaresan S, Pintar FA. Biomechanics of the cervical spine Part 2. Cervical spine soft tissue responses and biomechanical modeling. *Clin Biomech (Bristol, Avon).* 2001;16(1):1–27.
39. Lee SH, Im YJ, Kim KT, Kim YH, Park WM, Kim K. Comparison of cervical spine biomechanics after fixed- and mobile-core artificial disc replacement: a finite element analysis. *Spine (Phila Pa 1976).* 2011;36(9):700–8.
40. Hussain M, Natarajan RN, Fayyazi AH, Braaksmas BR, Andersson GB, An HS. Screw angulation affects bone-screw stresses and bone graft load sharing in anterior cervical corpectomy fusion with a rigid screw-plate construct: a finite element model study. *Spine J.* 2009;9(12):1016–23.
41. Tchako A, Sadegh AM. Stress changes in intervertebral discs of the cervical spine due to partial discectomies and fusion. *J Biomech Eng.* 2009;131(5):051013.
42. Wang Z, Zhao H, Liu JM, Chao R, Chen TB, Tan LW, Zhu F, Zhao JH, Liu P. Biomechanics of anterior plating failure in treating distractive flexion injury in the caudal subaxial cervical spine. *Clin Biomech (Bristol, Avon).* 2017;50:130–8.
43. Womack W, Woldtvedt D, Puttlitz CM. Lower cervical spine facet cartilage thickness mapping. *Osteoarthr Cartil.* 2008;16(9):1018–23.
44. Miura T, Panjabi MM, Cripton PA. A method to simulate in vivo cervical spine kinematics using in vitro compressive preload. *Spine (Phila Pa 1976).* 2002;27(1):43–8.
45. Wheelton JA, Pintar FA, Knowles S, Yoganandan N. Experimental flexion/extension data corridors for validation of finite element models of the young, normal cervical spine. *J Biomech.* 2006;39(2):375–80.
46. Yoganandan N, Pintar FA, Stemper BD, Wolfla CE, Shender BS, Paskoff G. Level-dependent coronal and axial moment-rotation corridors of degeneration-free cervical spines in lateral flexion. *J Bone Joint Surg Am.* 2007;89(5):1066–74.
47. Yoganandan N, Stemper BD, Pintar FA, Baisden JL, Shender BS, Paskoff G. Normative segment-specific axial and coronal angulation corridors of subaxial cervical column in axial rotation. *Spine (Phila Pa 1976).* 2008;33(5):490–6.
48. Patwardhan AG, Havey RM, Ghanayem AJ, Diener H, Meade KP, Dunlap B, Hodges SD. Load-carrying capacity of the human cervical spine in compression is increased under a follower load. *Spine (Phila Pa 1976).* 2000;25(12):1548–54.
49. Hussain M, Nassr A, Natarajan RN, An HS, Andersson GB. Biomechanics of adjacent segments after a multilevel cervical corpectomy using anterior, posterior, and combined anterior-posterior instrumentation techniques: a finite element model study. *Spine J.* 2013;13(6):689–96.
50. Hussain M, Nassr A, Natarajan RN, An HS, Andersson GB. Relationship between biomechanical changes at adjacent segments and number of fused bone grafts in multilevel cervical fusions: a finite element investigation. *J Neurosurg Spine.* 2014;20(1):22–9.
51. Hussain M, Natarajan RN, Chaudhary G, An HS, Andersson GB. Posterior facet load changes in adjacent segments due to moderate and severe degeneration in C5–C6 disc: a poroelastic C3–T1 finite element model study. *J Spinal Disord Tech.* 2012;25(4):218–25.
52. Setzer M, Eleraky M, Johnson WM, Aghayev K, Tran ND, Vronion FD. Biomechanical comparison of anterior cervical spine instrumentation techniques with and without supplemental posterior fusion after different corpectomy and discectomy combinations: laboratory investigation. *J Neurosurg Spine.* 2012;16(6):579–84.
53. Prasarn ML, Baria D, Milne E, Latta L, Sukovich W. Adjacent-level biomechanics after single versus multilevel cervical spine fusion. *J Neurosurg Spine.* 2012;16(2):172–7.
54. Song KJ, Choi BW, Jeon TS, Lee KB, Chang H. Adjacent segment degenerative disease: is it due to disease progression or a fusion-associated phenomenon? Comparison between segments adjacent to the fused and non-fused segments. *Eur Spine J.* 2011;20(11):1940–5.
55. David Kaye I, Hilibrand AS. Adjacent level disease-background and update based on disc replacement data. *Curr Rev Musculoskelet Med.* 2017;10(2):147–52.
56. Harrod CC, Hilibrand AS, Fischer DJ, Skelly AC. Adjacent segment pathology following cervical motion-sparing procedures or devices compared with fusion surgery: a systematic review. *Spine (Phila Pa 1976).* 2012;37(22 Suppl):S96–s112.
57. Setton LA, Chen J. Mechanobiology of the intervertebral disc and relevance to disc degeneration. *J Bone Joint Surg Am.* 2006;88(Suppl 2):52–7.
58. Setton LA, Chen J. Cell mechanics and mechanobiology in the intervertebral disc. *Spine (Phila Pa 1976).* 2004;29(23):2710–23.
59. Neidlinger-Wilke C, Wurtz K, Urban JP, Borm W, Arand M, Ignatius A, Wilke HJ, Claes LE. Regulation of gene expression in intervertebral disc cells by low and high hydrostatic pressure. *Eur Spine J.* 2006;15(Suppl 3):S372–8.
60. Stein MI, Nayak AN, Gaskins RB 3rd, Cabezas AF, Santoni BG, Castellvi AE. Biomechanics of an integrated interbody device versus ACDF anterior locking plate in a single-level cervical spine fusion construct. *Spine J.* 2014;14(1):128–36.
61. Scholz M, Reyes PM, Schleicher P, Sawa AG, Baek S, Kandziora F, Marciano FF, Crawford NR. A new stand-alone cervical anterior interbody fusion device: biomechanical comparison with established anterior cervical fixation devices. *Spine (Phila Pa 1976).* 2009;34(2):156–60.
62. Scholz M, Schnake KJ, Pingel A, Hoffmann R, Kandziora F. A new zero-profile implant for stand-alone anterior cervical interbody fusion. *Clin Orthop Relat Res.* 2011;469(3):666–73.
63. Sun Z, Liu Z, Hu W, Yang Y, Xiao X, Wang X. Zero-profile versus cage and plate in anterior cervical discectomy and fusion with a minimum 2 years of follow-up: a meta-analysis. *World Neurosurg.* 2018;120:e551–61.
64. Chen Y, Chen H, Cao P, Yuan W. Anterior cervical interbody fusion with the zero-P spacer: mid-term results of two-level fusion. *Eur Spine J.* 2015;24(8):1666–72.
65. Li Y, Hao D, He B, Wang X, Yan L. The efficiency of zero-profile implant in anterior cervical discectomy fusion: a prospective controlled long-term follow-up study. *J Spinal Disord Tech.* 2015;28(10):398–403.
66. Li Z, Zhao Y, Tang J, Ren D, Guo J, Wang H, Li L, Hou S. A comparison of a new zero-profile, stand-alone Fidji cervical cage and anterior cervical plate for single and multilevel ACDF: a minimum 2-year follow-up study. *Eur Spine J.* 2017;26(4):1129–39.
67. Chen Y, Liu Y, Chen H, Cao P, Yuan W. Comparison of curvature between the zero-P spacer and traditional cage and plate after 3-level anterior cervical discectomy and fusion: mid-term results. *Clin Spine Surg.* 2017;30(8):E1111–e1116.
68. Berg-Johansen B, Han M, Fields AJ, Liebenberg EC, Lim BJ, Larson PE, Gunduz-Demir C, Kazakia GJ, Krug R, Lotz JC. Cartilage endplate thickness variation measured by Ultrashort Echo-time MRI is associated with adjacent disc degeneration. *Spine.* 2018;43(10):E592–600.
69. Wu Y, Cisevski SE, Sachs BL, Pellegrini VD Jr, Kern MJ, Slate EH, Yao H. The region-dependent biomechanical and biochemical properties of bovine cartilaginous endplate. *J Biomech.* 2015;48(12):3185–91.

70. Zhao Y, Sun Y, Zhou F, Wang S, Zhang F, Pan S. Adjacent segment disease after anterior cervical decompression and fusion: analysis of risk factors on X-ray and magnetic resonance imaging. *Chin Med J*. 2014;127(22):3867–70.
71. Yu C, Mu X, Wei J, Chu Y, Liang B. In-depth analysis on influencing factors of adjacent segment degeneration after cervical fusion. *Med Sci Monit*. 2016;22:4902–10.
72. Goffin J, Geusens E, Vantomme N, Quintens E, Waerzeggers Y, Depreitere B, Van Calenbergh F, van Loon J. Long-term follow-up after interbody fusion of the cervical spine. *J Spinal Disord Tech*. 2004;17(2):79–85.
73. Wang H, Ma L, Yang D, Yang S, Ding W. Incidence and risk factors of postoperative adjacent segment degeneration following anterior decompression and instrumented fusion for degenerative disorders of the cervical spine. *World Neurosurg*. 2017;105:78–85.

Publisher's Note

Springer Nature remains neutral with regard to jurisdictional claims in published maps and institutional affiliations.

Ready to submit your research? Choose BMC and benefit from:

- fast, convenient online submission
- thorough peer review by experienced researchers in your field
- rapid publication on acceptance
- support for research data, including large and complex data types
- gold Open Access which fosters wider collaboration and increased citations
- maximum visibility for your research: over 100M website views per year

At BMC, research is always in progress.

Learn more biomedcentral.com/submissions

